Bioorganic & Medicinal Chemistry Letters 20 (2010) 5544–5547

Contents lists available at ScienceDirect

Bioorganic & Medicinal Chemistry Letters

journal homepage: www.elsevier.com/locate/bmcl

The discovery of an orally efficacious positive allosteric modulator of the calcium sensing receptor containing a dibenzylamine core

Paul E. Harrington [a,*], David J. St. Jean Jr. [a,*], Jeffrey Clarine [d], Thomas S. Coulter [e], Michael Croghan [a], Adam Davenport [e], James Davis [b], Chiara Ghiron [e], Jonathan Hutchinson [e], Michael G. Kelly [a], Fred Lott [b,†], Jenny Ying-Lin Lu [c], David Martin [b,‡], Sean Morony [b], Steve F. Poon [a], Elena Portero-Larragueta [e], Jeff D. Reagan [c], Kelly A. Regal [d,§], Andrew Tasker [a], Minghan Wang [b], Yuhua Yang [c], Guomin Yao [a], Qingping Zeng [a], Charles Henley III [b], Christopher Fotsch [a]

[a] Chemistry Research and Discovery, Amgen Inc., One Amgen Center Drive, Thousand Oaks, CA 91320, USA
[b] Metabolic Disorders, Amgen Inc., One Amgen Center Drive, Thousand Oaks, CA 91320, USA
[c] Metabolic Disorders, Amgen Inc., 1120 Veterans Boulevard, South San Francisco, CA 94080, USA
[d] Pharmacokinetics and Drug Metabolism, Amgen Inc., One Amgen Center Drive, Thousand Oaks, CA 91320, USA
[e] Evotec (UK) Ltd, 114 Milton Park, Abingdon, Oxfordshire OX14 4SA, UK

ARTICLE INFO

Article history:
Received 9 June 2010
Revised 13 July 2010
Accepted 15 July 2010
Available online 12 August 2010

Keywords:
Calcimimetic
Allosteric modulator

ABSTRACT

The discovery of a series of novel and orally efficacious type II calcimimetics, developed from the lead compound **1**, is described herein. Compound **22** suppressed plasma PTH levels relative to vehicle when dosed orally in a rat pharmacodynamic model.

The regulation of serum calcium ions is vital to a wide range of physiological processes. The mechanism by which the concentration of serum ionized calcium is controlled is complex. The parathyroid and thyroid glands, bone, kidney, and intestine all act in concert to tightly regulate the concentration of ionized calcium.[1] The calcium sensing receptor (CaSR) plays a fundamental role in the regulation of extracellular calcium within the physiological range of 1.1–1.3 mM.[2] The CaSR is a cell surface receptor that is part of the superfamily of G protein-coupled receptors (GPCR) and is comprised of 1078 amino acids with seven transmembrane domains. On parathyroid chief cells, the CaSR controls the secretion of parathyroid hormone (PTH), a hormone that is responsible for raising serum ionized calcium levels.

The concentration of extracellular ionized calcium is regulated via a feedback loop mechanism involving Ca^{2+} ions, the CaSR, and PTH. In response to low extracellular calcium levels (low Ca^{2+}), the chief cells of the parathyroid secrete PTH from intracellular vesicles. PTH then raises extracellular Ca^{2+} by stimulating calcium resorption from the bone and enhancing calcium reabsorption from the kidney and gut. However, when extracellular Ca^{2+} concentrations are increased, the CaSR is activated, and secretion of PTH is suppressed. Thus, the CaSR acts as a biological brake, being activated during times of high extracellular Ca^{2+}, which keeps the parathyroid from secreting excess PTH. Ligands that mimic the effect Ca^{2+} has on the CaSR are called calcimimetics.[3]

Type I calcimimetics such as inorganic[4] and organic polycations directly activate the CaSR in the form of classic agonists. Type II calcimimetics function as positive allosteric modulators of the CaSR and thus increase the sensitivity of the CaSR to extracellular calcium. Cinacalcet HCl (Sensipar®, Mimpara®), a type II calcimimetic, is on the market in certain territories for diseases related to hypercalcemia;[5] which include primary and secondary hyperparathyroidism (1HPT and 2HPT) and parathyroid carcinoma.

In vitro screening for novel type II calcimimetics was performed using a cell-based assay in the presence and absence of extracellular Ca^{2+}.[6] Compounds which activated the receptor only in the presence of extracellular Ca^{2+} were positive allosteric activators of the CaSR. Benzyl amine **1** (CaSR EC_{50} = 1.2 μM, Fig. 1) was identified as a lead candidate for further optimization.

Initial SAR focused on the B-ring analogs **1**–**4**. The synthesis of the benzyl amine compounds **1**–**9** is shown in Scheme 1.[7] Reductive

---

* Corresponding authors.
E-mail address: pharring@amgen.com (P.E. Harrington).
[†] Present address: Sundance Ranch, 12955 Back Canyon Road, Caliente, CA 93518, USA.
[‡] Present address: South San Francisco, CA 94080, USA.
[§] Present address: Array BioPharma Inc., Boulder, CO 80301, USA.

0960-894X/$ - see front matter © 2010 Elsevier Ltd. All rights reserved.
doi:10.1016/j.bmcl.2010.07.060

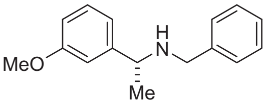

1

CaR EC$_{50}$ = 1.2 ± 0.3 μM

Figure 1. Benzyl amine **1**.

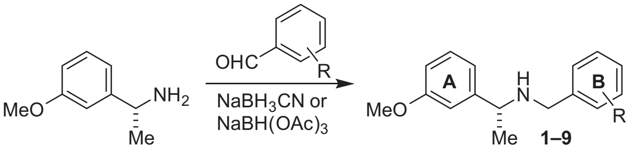

Scheme 1. Synthesis of benzyl amines **1–9**.

Table 1
SAR of B-ring analogs **1–4**

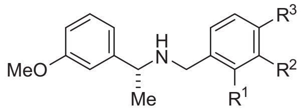

Compound	R^1	R^2	R^3	CaSR EC$_{50}$[a] (μM)	CaSR max[a,b] (%)
1	H	H	H	1.2 ± 0.3[c]	24 ± 4[c]
2	Cl	H	H	3.7 ± 1.5	110 ± 69
3	H	*o*-ClPh	H	0.35 ± 0.20	97 ± 11
4	H	H	OMe	0.37 ± 0.02	88 ± 2

[a] Mean ± SD with $n \geqslant 3$.

[b] Max (%) is the ratio of the compound induced FLIPR response divided by the maximum FLIPR response induced by a saturating dose of $CaCl_2$ (10 mM) multiplied by 100.

[c] $n = 2$.

Table 2
SAR of C-ring biphenyl analogs **5–9**

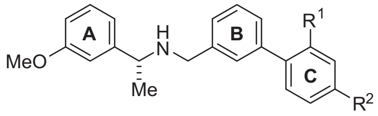

Compound	R^1	R^2	CaSR EC$_{50}$[a] (μM)	CaSR max[a] (%)
5	F	H	2.7 ± 2.0	109 ± 40
6	Me	H	2.2 ± 0.3	93 ± 7
7	OMe	H	1.4 ± 0.2	92 ± 6
8	H	OMe	0.87 ± 0.05	95 ± 4
9	H	CF_3	0.62 ± 0.08	86 ± 9

[a] Mean ± SD with $n \geqslant 3$.

amination[8] of the commercially available aldehydes with (*R*)-1-(3-methoxyphenyl)ethanamine yielded **1–9** in a single step.

The potency and percent activation in the CaSR assay of the B-ring analogs **1–4** is shown in Table 1. Both the unsubstituted phenyl analog **1** and the chloro analog **2** had EC$_{50}$ >1 μM. In addition, **1** had a lower maximal activation. However, compound **3**, with the B-ring *ortho*-chlorophenyl substituent, was significantly more potent than either **1** or **2** with an EC$_{50}$ = 0.35 μM. Furthermore, compound **4** (EC$_{50}$ = 0.37 μM) was also more potent than the parent compound **1**. These results provided two avenues, B-ring *meta* aryl and B-ring *para* substitution, for further SAR studies and opportunities to further improve the dibenzylamine scaffold.

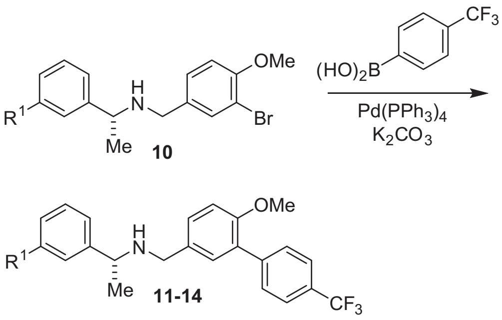

Scheme 2. Synthesis of biphenyl amines **11–14**.

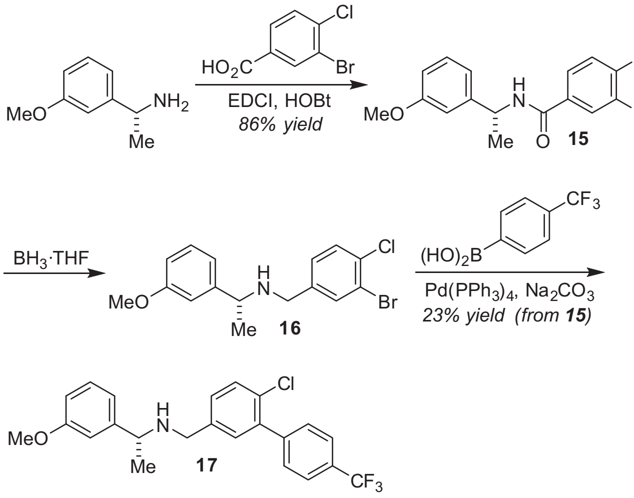

Scheme 3. Synthesis of chlorobiphenyl analog **17**.

Table 2 highlights the results from the optimization of the C-ring phenyl substituent. Compounds **6–7** were prepared to further examine the SAR at the *ortho* position (R^1) of the C-ring. Within this limited set of compounds, no improvement in potency relative to **3** was achieved. However, the C-ring *para* substituted analogs, methoxy **8** and trifluoromethyl **9**, had an EC$_{50}$ <1 μM.

Having established the importance of the C-ring phenyl for in vitro potency, we sought to further improve these compounds by adding a B-ring methoxy group, a functional group that improved the activity of analog **4** relative to **1**. The *para*-methoxy analogs **11–14** were prepared as shown in Scheme 2. Bromide **10** was prepared through a reductive amination (Scheme 1). Palladium catalyzed Suzuki–Miyaura coupling of **10** with the corresponding boronic acid yielded biphenyls **11–14**. The B-ring *para*-chloro analog **17** was prepared by the route highlighted in Scheme 3. Amide coupling of (*R*)-1-(3-methoxyphenyl)ethanamine with 3-bromo-4-chlorobenzoic acid gave **15** in 86% yield. Amide reduction with BH_3·THF followed by Suzuki–Miyaura coupling provided **17**.

Table 3 summarizes the SAR for the substituted biphenyl analogs **11–14** and **17**. Significant in vitro potency gains were achieved by combining the C-ring *para*-trifluoromethylphenyl with the B-ring *para*-methoxy substituents. For example, compound **11** (EC$_{50}$ = 0.023 μM) was significantly more potent than either **4** or **9** thus confirming the additive effect of the C-ring *para*-trifluoromethylphenyl and B-ring *para*-methoxy groups. However, the B-ring *para*-chloro analog **17** was approximately 10-fold less potent than the corresponding methoxy compound **11**. Optimization of the A-ring revealed that phenyl (**12**, EC$_{50}$ = 0.027 μM) and *meta*-fluoro

Table 3
SAR of substituted biphenyl analogs **11**–**14** and **17**

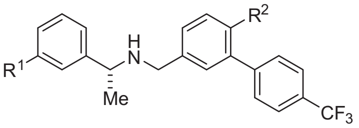

Compound	R^1	R^2	CaSR EC$_{50}$[a] (μM)	CaSR max[a] (%)
11	OMe	OMe	0.023 ± 0.009	87 ± 1
12	H	OMe	0.027 ± 0.017	92 ± 9
13	F	OMe	0.037 ± 0.046	99 ± 10
14[b]	Me	OMe	0.16 ± 0.10	99 ± 13
17	OMe	Cl	0.28 ± 0.02	93 ± 11

[a] Mean ± SD with $n \geqslant 3$.
[b] Racemic.

Table 4
Rat pharmacokinetic parameters for compounds **11** and **12** administered iv

Compound	Dose[a] (mg/kg)	CL (L/h/kg)	V_{ss} (L/kg)	$t_{1/2}$ (h)	AUC$_{0-\text{inf}}$ (ng h/mL)
11	3.5	4.0	28	4.9	886
12	3.0	3.3	22	6.1	905

[a] Pharmacokinetic studies were conducted in male Sprague–Dawley rats and were administered in 20% Captisol/water.

(**13**, EC$_{50}$ = 0.037 μM) were both more active than the *meta*-methyl analog (**14**, EC$_{50}$ = 0.16 μM).

The pharmacokinetic profiles of the two most promising analogs, **11** and **12**, are shown in Table 4. Unfortunately, both compounds exhibited clearance at or above liver blood flow in male Sprague–Dawley rats when dosed intravenously. Despite the high clearance, the high volume of distribution for both **11** and **12** resulted in half-lives of 4.9 and 6.1 h, respectively. With these results, we sought to decrease the in vivo clearance of **12** by blocking potential sites of metabolism. These positions included one of the benzylic carbons, the *para*-position on the A-ring, and the B-ring methoxy, which were predicted as metabolically labile positions using MetaSite software.[9] Based on this theory, fluorinated and substituted derivatives were synthesized via the routes described in Scheme 4. Palladium catalyzed Suzuki–Miyaura coupling[10] produced the functionalized aldehydes or acetophenone (**18**–**20**) in high yields. Reductive amination using standard conditions delivered analogs **21** and **24**. Methylated derivatives **22** and **23** were synthesized in an analogous manner; although the reductive amination required pre-formation of the acetophenone imine with TiCl$_4$.[11] The diastereomeric ratio was 14:1 favoring the *R*,*R*-diastereomer (**22**). The stereochemistry of the major diastereomer was confirmed by single crystal X-ray analysis.

Table 5 summarizes the SAR for analogs **21**–**24**. An attempt to incorporate a fluorine at the *para* position of the A-ring resulted in decreased activity relative to **12**. In addition, the B-ring trifluoromethyl compound **24** was less active than **12**. However, incorporation of a methyl group at the unsubstituted benzylic carbon (R^3) resulted in a compound equipotent to **12**. There was a strong stereochemical preference for the *R*,*R*-diastereomer (cf. analog **22** vs **23**, which had EC$_{50}$ values of 0.017 and 3.0 μM, respectively).

The pharmacokinetic profile of **22** is shown in Table 6. Relative to analog **12**, the clearance was significantly improved. The high V_{ss} and the moderate clearance led to a significantly higher AUC relative to compound **12**. Given the promising in vitro and in vivo profile of **22**, along with good rat oral bioavailability[12] (%F = 60, C_{max} = 90 ng/mL), this molecule was progressed to a rat pharmacodynamic model to access its ability to lower PTH levels.

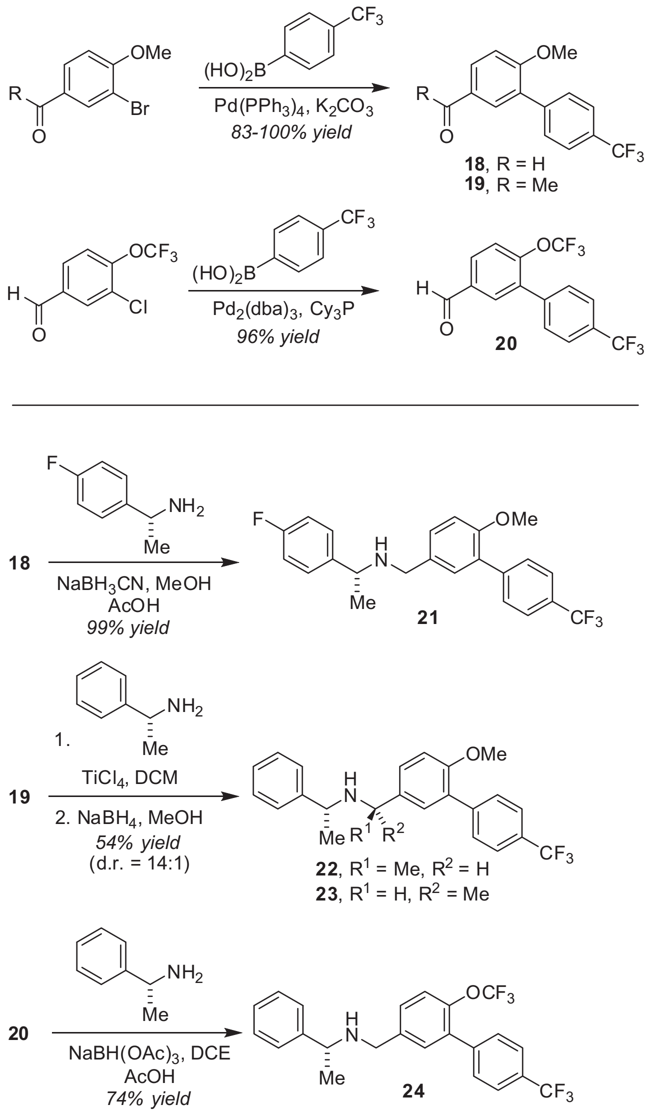

Scheme 4. Synthesis of analogs **21**–**24**.

Table 5
SAR of fluorinated and substituted analogs of **12**

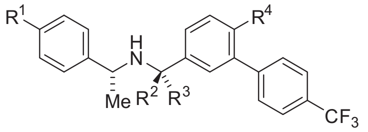

Compound	R^1	R^2	R^3	R^4	CaSR EC$_{50}$[a] (μM)	CaSR max[a] (%)
21	F	H	H	OMe	0.058 ± 0.042	87 ± 13
22	H	Me	H	OMe	0.017 ± 0.022	94 ± 8
23	H	H	Me	OMe	3.0 ± 2.9[b]	163 ± 103[b]
24	H	H	H	OCF$_3$	0.11[c]	74[c]

[a] Mean ± SD with $n \geqslant 3$.
[b] n = 2.
[c] n = 1.

In this study, compound **22** was dosed orally to normal male Sprague–Dawley rats to determine the effect on circulating PTH at varying doses (0.3, 1, 3 mg/kg).[13] After a single 0.3 mg/kg (green line) dose, plasma PTH levels were reduced relative to vehicle (black line) out to 8 h (Fig. 2). At the highest dose (3 mg/kg, red line) PTH levels were significantly suppressed after 1 day.

Table 6
Rat pharmacokinetic parameters for compound **22** administered iv[a]

Compound	CL (L/h/kg)	V_{ss} (L/kg)	$t_{1/2}$ (h)	AUC_{0-inf} (ng h/mL)
22	1.6	18	9.3	2020

[a] Pharmacokinetic study was conducted in male Sprague–Dawley rats and was administered in 100% DMSO at 3 mg/kg.

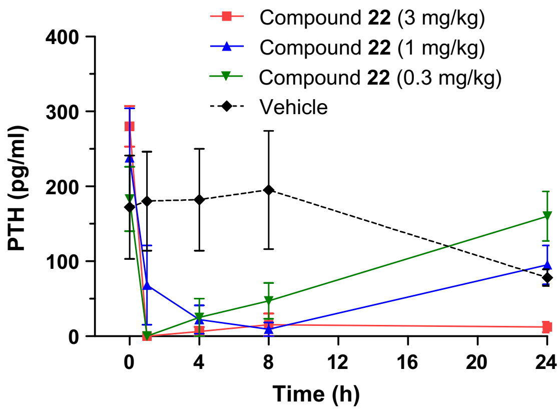

Figure 2. Dose–response effects of **22** (0.3, 1, and 3 mg/kg) or vehicle (2% HPMC/1% Tween 80/5% Captisol) on plasma parathyroid hormone (PTH) following oral administration to normal male Sprague–Dawley rats ($n = 4$/group).

In conclusion, a novel series of type II calcimimetics has been discovered. Although analog **12** possessed excellent in vitro potency relative to **1** ($EC_{50} = 0.027$ vs 1.2 μM), it displayed high in vivo clearance in rats (CL = 3.3 L/h/kg). Systematic attempts to improve clearance or slow metabolism led to the discovery of analog **22**, which maintained the in vitro potency of **12** while significantly improving the in vivo clearance. In a rat pharmacodynamic model, compound **22** showed a decrease in circulating PTH levels in a dose dependent manner.

Acknowledgments

We acknowledge Roger Zanon and Yiping Wu for their assistance with formulations and rat pharmacokinetics, respectively. The authors also thank Rashid Syed for providing X-ray crystallographic support.

References and notes

1. (a) Brown, E. M. *Physiol. Rev.* **1991**, *71*, 371; (b) Mihai, R.; Farndon, J. R. *Br. J. Anaesth.* **2000**, *85*, 29; (c) Silver, J.; Kilav, R.; Naveh-Many, T. *Am. J. Physiol. Renal Physiol.* **2002**, *283*, F367; (d) Kurokawa, K. *Kidney Int.* **1994**, *44*, S97; (e) Dempster, D. W.; Cosman, F.; Parisien, M.; Shen, V.; Lindsay, R. *Endocr. Rev.* **1993**, *14*, 690.
2. (a) Brown, E. M.; Gamba, G.; Riccardi, D.; Lombardi, M.; Butters, R.; Kifor, O.; Sun, A.; Hediger, M. A.; Lytton, J.; Hebert, S. C. *Nature* **1993**, *366*, 575; (b) Brown, E. M.; MacLeod, R. J. *Physiol. Rev.* **2001**, *81*, 239; (c) Hofer, A. M.; Brown, E. M. *Nat. Rev. Mol. Cell Biol.* **2003**, *4*, 530.
3. (a) Nagano, N. *Pharmacol. Ther.* **2006**, *109*, 339; (b) Urena, P.; Frazao, J. M. *Kidney Int.* **2003**, *63*, S91; (c) Steddon, S. J.; Cunningham, J. *Lancet* **2005**, *365*, 2237; (d) Nemeth, E. F. In *Principles of Bone Biology*; Bilezikian, J. P., Raisz, L. G., Rodan, G. A., Eds.; Academic Press: San Diego, 2002; pp 1339–1359; (e) Hebert, S. C. *Annu. Rev. Med.* **2006**, *57*, 349; (f) Harrington, P. E.; Fotsch, C. *Curr. Med. Chem.* **2007**, *14*, 3027.
4. Nemeth, E. F.; Scarpa, A. *J. Biol. Chem.* **1987**, *262*, 5188.
5. Balfour, J. A. B.; Scott, L. J. *Drugs* **2005**, *65*, 271.
6. (a) Nemeth, E. F.; Heaton, W. H.; Miller, M.; Fox, J.; Balandrin, M. F.; Van Wagenen, B. C.; Colloton, M.; Karbon, W.; Scherrer, J.; Shatzen, E.; Rishton, G.; Scully, S.; Qi, M.; Harris, R.; Lacey, D.; Martin, D. *J. Pharmacol. Exp. Ther.* **2004**, *308*, 627; (b) The following compounds had CaSR EC_{50} values <5 μM in the absence of extracellular Ca^{2+}: **3** (1.7 μM), **11** (0.72 μM), **13** (1.3 μM), **14** (0.43 μM), **21** (1.7 μM), **22** (2.1 μM). All remaining compounds had CaSR EC_{50} values >5 μM in the absence of extracellular Ca^{2}.
7. All compounds were characterized by ^{1}H NMR and LC/MS and their purity was determined to be >95% by reverse phase HPLC.
8. Abdel-Magid, A. F.; Carson, K. G.; Harris, B. D.; Maryanoff, C. A.; Shah, R. D. *J. Org. Chem.* **1996**, *61*, 3849.
9. Cruciani, G.; Carosati, E.; De Boeck, B.; Ethirajulu, K.; Mackie, C.; Howe, T.; Vianello, R. *J. Med. Chem.* **2005**, *48*, 6970.
10. Kudo, N.; Perseghini, M.; Fu, G. C. *Angew. Chem., Int. Ed.* **2006**, *45*, 1282.
11. Bringmann, G.; Geisler, J.-P. *Tetrahedron Lett.* **1989**, *30*, 317.
12. Oral pharmacokinetic study was conducted in male Sprague–Dawley rats and was administered in 2% HPMC/1% Tween 80/5% Captisol in water at 3 mg/kg.
13. The concentration of **22** at 1 h was: 7 ± 1 ng/mL (0.3 mpk), 17 ± 8 ng/mL (1 mpk), and 37 ± 12 ng/mL (3 mpk).